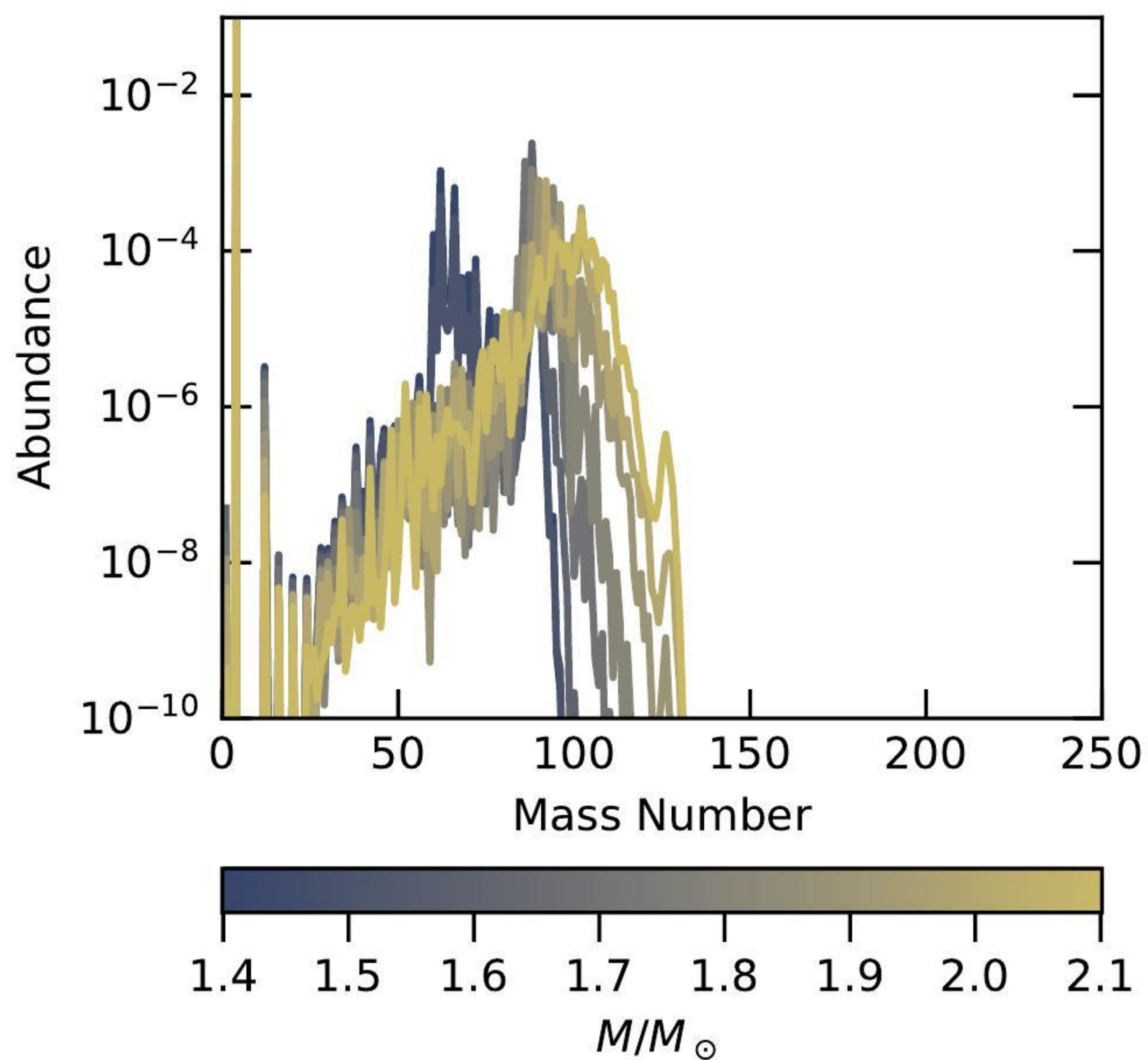


**Figure 2.** Entropy versus radius for PNSs of varying mass, with a fixed total neutrino luminosity of  $6 \times 10^{51} \text{ erg s}^{-1}$ , and  $L_w = 0$ . We find comparable behavior to Wanajo (2013). The approximate beginning of seed formation for each model is marked with a square.



**Figure 3.** Final abundances in the absence of wave effects (i.e.  $L_w = 0$ ), with  $L_\nu = 6 \times 10^{51} \text{ erg s}^{-1}$  and PNS masses ranging from 1.4-2.1  $M_\odot$ . We find that no r-processing takes place for proto-neutron stars of reasonable masses with  $Y_{e,\text{eq}} = 0.48$ , when wave effects are excluded.

required for an r-process. The included general relativistic corrections to the wind equations increase the entropy as expected (Cardall & Fuller 1997; Thompson et al. 2001). Nucleosynthesis results for these NDW profiles assuming  $Y_{e,\text{eq}} = 0.48$  are shown in figure 3. For these models without gravito-acoustic wave heating, the electron fraction at  $T = 0.5 \text{ MeV}$  is nearly equal to the chosen  $Y_{e,\text{eq}}$ . In contrast to

Wanajo (2013), we find that even for the highest neutron star masses, no r-processing takes place in these winds.

## 5.2 The Impact of Gravito-Acoustic Waves on the NDW

### 5.2.1 Wind Dynamics

We now consider the impact of gravito-acoustic waves on the dynamics of the NDW. As is described above, the presence of these waves in the wind can accelerate the NDW by purely mechanical effects and can deposit heat in the wind once the waves shock. Since  $L_w$  should scale with  $L_\nu$  (see section 2), we present our results in terms of the ratio  $L_w/L_\nu$ . In figure 4, properties of steady state NDW models with  $L_\nu = 3 \times 10^{52} \text{ erg s}^{-1}$ ,  $Y_{e,\text{eq}} = 0.48$ ,  $M_{\text{NS}} = 1.5 M_\odot$ ,  $\omega = 2 \times 10^3 \text{ rad s}^{-1}$ , and varied  $L_w/L_\nu$  are shown. Results for  $M_{\text{NS}} = 1.9 M_\odot$  are qualitatively similar, albeit with higher final entropies. Seed formation begins approximately when the temperature in the wind drops to  $T = 0.5 \text{ MeV}$  (Qian & Woosley 1996), which is marked in figures with a square. Clearly, above  $L_w/L_\nu \approx 10^{-5}$ , the inclusion of wave effects has a significant impact on the dynamics of the wind. Although  $L_w$  in these models is a relatively small fraction of the total neutrino luminosity, it is a large fraction of the neutrino energy that couples to the wind,  $\dot{Q}_\nu$  (see equation 2). At small radii, before the waves shock, they accelerate the NDW but do not provide any heating. This results in increasing velocities with  $L_w/L_\nu$ , and therefore lower densities at a given radius by the relation  $\dot{M}_{\text{NS}} = 4\pi r^2 e^\Lambda W \rho v$ . Additionally, since the acceleration of the wind is no longer provided solely by neutrino heating, the amount of neutrino heating that occurs is lowered, which results in both lower entropies before the wave-heating activation radius, and in lower electron fractions at all points in the wind. As the wave contribution increases, fewer neutrino captures are required to unbind material from the potential well of the PNS and the NDW is accelerated to higher velocities at smaller radii. Both of these effects work to reduce the number of weak interactions in the wind and prevent the electron fraction in the wind from reaching  $Y_{e,\text{eq}}$ , which results in more neutron-rich conditions at the beginning of nucleosynthesis. The changes in  $Y_e$  begin prior to the waves forming weak shocks, indicating that the wave stress, rather than shock heating, is the primary contributor. These effects will therefore be present regardless of any uncertainty in the shock heating mechanism. We observe a spike in  $Y_e$  at small radii due to electron-positron capture when degeneracy is lifted at high temperatures. The electron fraction then relaxes towards  $Y_{e,\text{eq}}$ , but may not reach it due to the wave contributions.

Subsequent to the waves shocking, the entropy rapidly increases in all models. Shock formation occurs at temperatures between 2 and 10 GK depending on  $L_w/L_\nu$  (and  $\omega$ , see figure 5). The extra entropy production provided by  $\dot{q}_w$  is large compared to neutrino heating because of the low temperatures at which it occurs compared to the temperatures where the bulk of the neutrino heating takes place ( $\sim 30 \text{ GK}$  in our simulations). For the largest  $L_w/L_\nu$ , the entropy can reach asymptotic values of 300, which is quite large compared to even the largest entropies found for models that do not experience wave heating (see section 5.1). Nevertheless, a significant amount of the entropy production occurs during or after the temperatures over which seed nuclei for the r-process are produced ( $\sim 2 - 8 \text{ GK}$ ). Therefore, estimating the likelihood of r-process nucleosynthesis from the often used metric  $s^3/\tau_d$  (see Hoffman et al. 1997) is difficult as  $s$  is no longer nearly constant while seed production occurs. Before the shock formation radius, the waves reduce both  $s$  and